ELSEVIER

Ceramics International 29 (2003) 447–453

CERAMICS INTERNATIONAL

www.elsevier.com/locate/ceramint

# Sinterable ferroelectric glass-ceramics containing (Sr, Ba)$Nb_2O_6$ crystals

Jiin-Jyh Shyu*, Chia-Hua Chen

*Department of Materials Engineering, Tatung University, Taipei 104, Taiwan, ROC*

Received 10 May 2002; received in revised form 18 August 2002; accepted 20 September 2002

**Abstract**

The densification, crystallization, and dielectric/ferroelectric properties of a SrO–BaO–$Nb_2O_5$–$SiO_2$ glass-ceramic were investigated. Glass-ceramics containing (Sr, Ba)$Nb_2O_6$ tungsten bronze as the major crystalline phase can be sintered below 1000 °C. The good sinterability is attributed to that the major crystallization process occurred after the sintering of the glass powder compact. The variations of dielectric properties with sintering temperature and test frequency can be explained qualitatively by the amount of SBN phase formed. The maximum dielectric constant at 1 kHz is about 351 for the glass-ceramic sintered at 1000 °C. The existence of ferroelectricity is verified for the present glass-ceramic. The values of the remanent polarization and the coercive field are about 0.15 μC/cm$^2$ and 4.5 kV/cm, respectively, for the glass-ceramic sintered at 1000 °C.


*Keywords:* A. Sintering; C. Ferroelectric property; D. Glass ceramics; D. Niobates

## 1. Introduction

Controlled crystallization in glasses has led to the development of glass-ceramic materials with pore-free, fine-grained microstructure and specific properties. Much of the work in the field of glass-ceramics has been done on the thermal and mechanical properties. On the other hand, fewer investigations were reported on the high-permittivity glass-ceramics containing a ferroelectric phase, such as $BaTiO_3$ [1–4], $PbTiO_3$ [5–10], $LiTaO_3$ [11], $LiNbO_3$ [12–15], $NaNbO_3$ [11,15–18], $KNbO_3$ [11,19,20], and (Sr, Ba)$Nb_2O_6$ [21,22].

In our previous paper [22], we have reported on the crystallization of (Sr, Ba)$Nb_2O_6$ tungsten-bronze phase from SrO–BaO–$Nb_2O_5$–$SiO_2$ monolithic glasses, as well as the dielectric properties of the resulting glass-ceramics. It is known that glass-ceramic materials can also be produced by sintering and crystallization of glass powder. The shaped powder compacts are subjected to heat treatment leading to densification and crystallization. This technology permits manufacture of small quantities of products with complex shapes using ordinary ceramic-forming methods, for example, dry pressing, slip casting, tape casting, screen printing, extrusion, and injection molding [23].

It is well known that glass powders densify by viscous coalescence. However, most crystallizable glass powders are difficult to sinter because of the large surface area for nucleation, promoting crystal growth from the surface of every glass particle toward the center and inhibiting effective sintering to achieve full density [24,25]. In the present study, the sinterability of the SrO–BaO–$Nb_2O_5$–$SiO_2$ glass-ceramics containing ferroelectric (Sr, Ba)$Nb_2O_6$ phase has been demonstrated.

## 2. Experimental procedure

### 2.1. Sample preparation

A mixture of the mol% composition 22.5SrO, 22.5BaO, 15$Nb_2O_5$, 40$SiO_2$ was prepared from reagent-grade $SrCO_3$, $BaCO_3$, $Nb_2O_5$, and $SiO_2$. It was melted in a platinum crucible for 6 h at 1600 °C. The melt was quenched into frit form by being poured into deionized water. The dried frits were crushed in an alumina-lined

* Corresponding author. Tel.: +886-2-2586-6440; fax: +886-2-2593-6897.

*E-mail address:* jjshyu@ttu.edu.tw (J.-J. Shyu).

0272-8842/03/$30.00 
PII: S0272-8842(02)00186-4

mortar grinder (model RMO, F. Kurt Retsch GmbH & Co. KG, Germany) until the powder passed through 100 mesh. The crushed glass powder was then milled for 48 h in an yittria stabilized zirconia (YSZ)-lined mill containing YSZ balls, poly(vinyl alcohol), and alcohol. The resulting slurry was dried and screened (60 mesh). The resulting particle size for the glass powder was measured with a particle-size analyzer (model MSE02SM, Malvern Instruments Ltd., Worcestershire, UK) and was about 2.5 μm. The green compacts were uniaxially pressed in a 10 mm diameter steel die lubricated with a thin layer of stearic acid. The average green density was about 2.50 g/cm$^3$. The green compacts were prefired at a heating rate of 10 K/min to 500 °C and held for 2 h in air. The samples were then sintered in air at the selected temperatures between 700 and 1000 °C for 6 h, at a heating rate of 10 K/min, then furnace cooled.

### 2.2. Characterization

The diameter shrinkages and bulk densities of the sintered samples were measured by micrometer. Phase identification was conducted by X-ray diffraction (XRD) analysis. Measurements were performed on a diffractometer (Model D5000, Siemens, Karlsruhe, Germany) with Cu$K_\alpha$ radiation and a Ni filter. The operating power was 40 kV and 20 mA. A sampling interval of 0.05° (2$\theta$) was used. The sintered samples were polished, etched with a 0.5 wt% HF solution at 25 °C for 2 s, and then coated with a thin film of gold for scanning electron microscopy (SEM) observations.

Crystallized samples were gold electroded by sputtering for the dielectric and ferroelectric measurements.

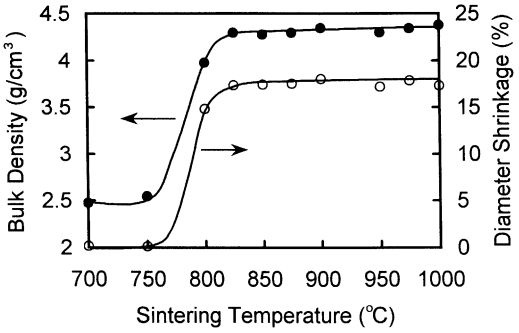


Fig. 1. Bulk density and diameter shrinkage as a function of sintering temperature.

The frequency dependencies of relative dielectric constant and dielectric loss tangent were measured by an LCR meter (HP 4284A, Hewlett-Packard, Tokyo, Japan) at room temperature with an oscillating voltage of 1 V in the frequency range 20 Hz to 1 MHz. The *P–E* hysteresis loop was observed at room temperature using a home-built modified Sawyer-Tower circuit with 60 Hz sinusoidal field. The sample was dipped in silicone oil during the measurement.

## 3. Results and discussion

Fig. 1 shows the diameter shrinkage and bulk density as a function of sintering temperature for the sintered bodies. Densification was not observed at 700–750 °C and remarkable densification occurred when the sintering temperature was increased to 800 °C. In the range of 825 to 1000 °C, the degree of densification was saturated. Curling of the sample was observed at temperatures $\geqslant$1100 °C.

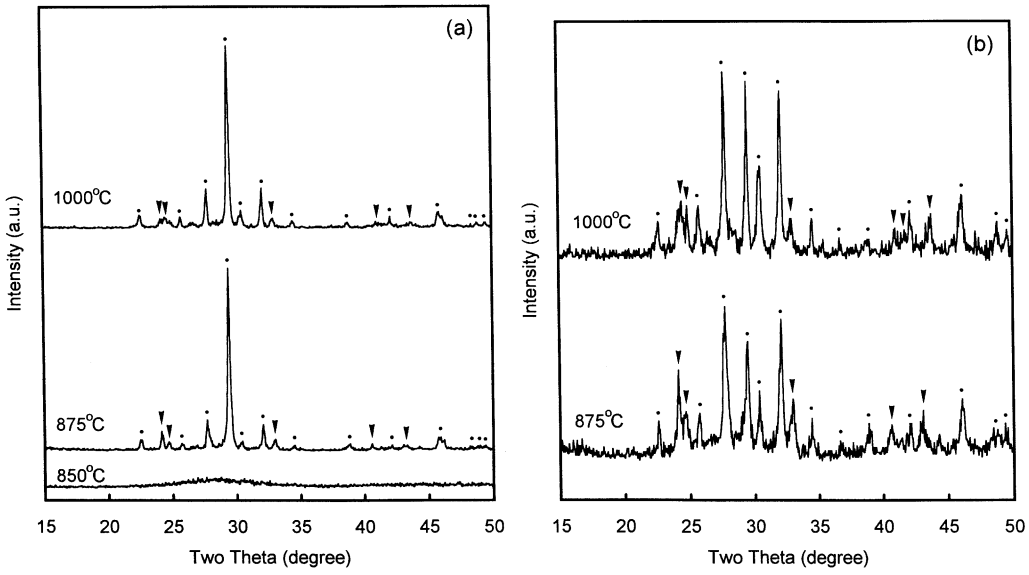


Fig. 2. XRD patterns of the (a) as-sintered and (b) polished surfaces for the samples sintered at various temperatures. (●: SBN, ▼: $B_2S_3$).

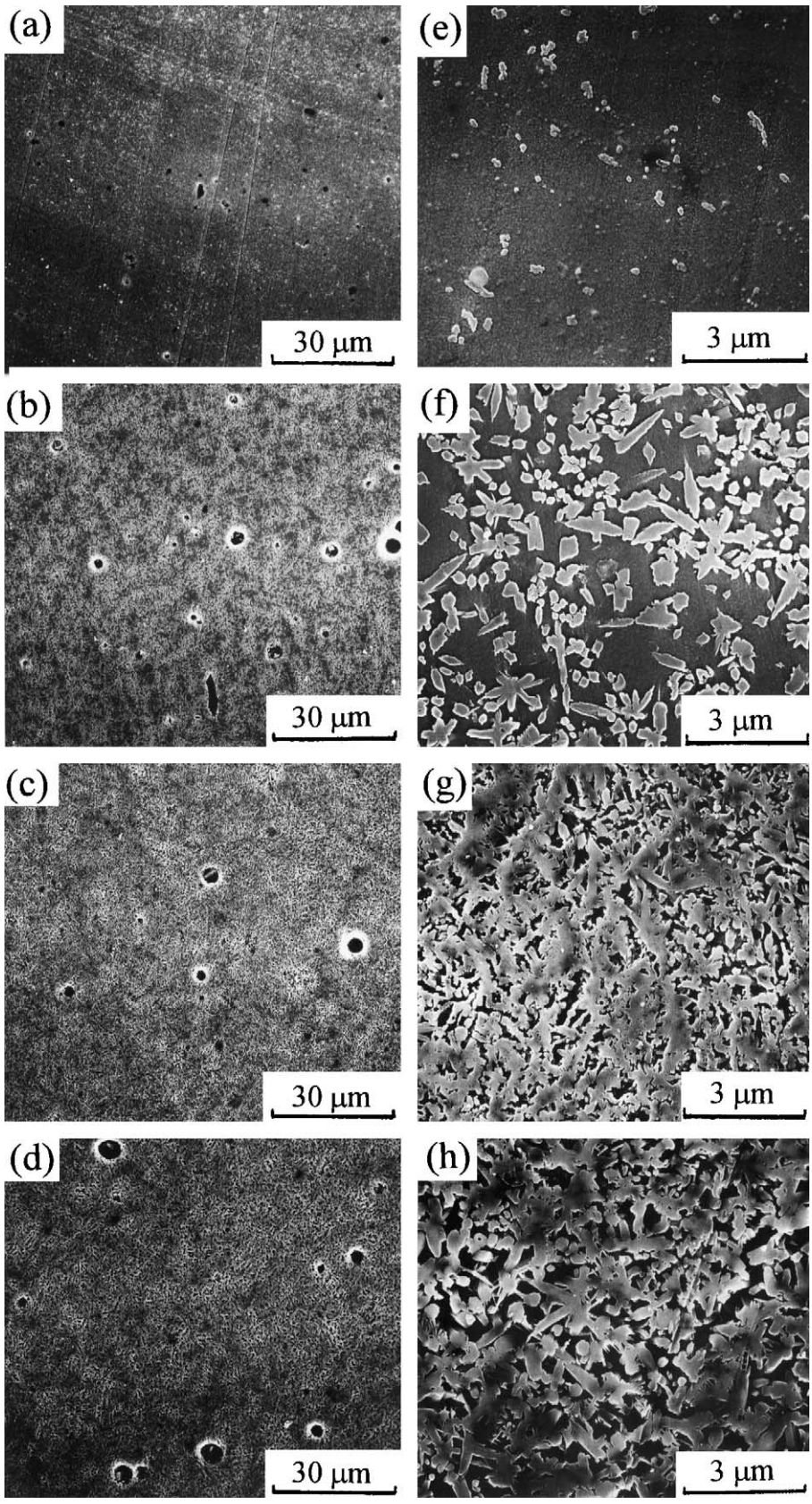


Fig. 3. SEM pictures showing the microstructures of the bulk regions of the samples sintered at (a)(e) 825 °C, (b)(f) 850 °C, (c)(g) 900 °C, and (d)(h) 1000 °C.

Fig. 2(a) and (b) shows the typical XRD patterns of the as-sintered and polished surfaces, respectively, for the sintered samples. It can be seen in Fig. 2(a) that the samples were still amorphous at 850 °C. In the range of 875–1000 °C, (Sr, Ba)$Nb_2O_6$ phase (denoted as SBN) and a phase most likely corresponding to $Ba_2Si_3O_8$ (JCPDS # 27-1035, denoted as $B_2S_3$) were observed. It can be seen that there is a strong (410) preferred orientation of SBN phase ($2\theta \approx 29.6°$) on the as-sintered surface. After removing the free surface by polished the sample [Fig. 2(b)], the texture was drastically vanished. This result illustrates that a thin layer of preferred orientation has developed on the sample surface. This phenomenon of surface texture can usually be seen in other glass-ceramic systems [26]. However, it is not clear why the surface-nucleated SBN crystals exhibited the earlier mentioned preferred orientation. Moreover, according to Fig. 2(b), some degree of the broad scattering intensity ($2\theta \approx 20$–$35°$), which is associated with residual glass, still remained at 875 °C. However, the broad scattering intensity disappeared at 1000 °C. The earlier results indicate that the crystallization processes mainly occurred at 875 °C and still proceeded at the higher temperatures.

The microstructures of the samples with the higher sintered densities were observed. Fig. 3(a)–(d) shows the typical microstructures for the samples sintered at 825–1000 °C to show the pore morphology. The high degree of densification is verified. The pores revealed a spherical shape, which can usually be observed in viscous sintering of glass powder compacts. Moreover, the major pore-growth occurred when the temperature was increased from 825 to 850 °C. This result can be explained by the low total-viscosity of the sample in this temperature range, because the remarkable crystallization process has not taken place (Fig. 2). When the sintering temperature was increased to $\geqslant$875 °C, the glass content was obviously reduced due to significant crystallization (Fig. 2). Therefore, the pore growth process ceased.

Fig. 3(e)–(h) are the enlarged microstructures to show the crystal morphology. Small SBN crystals precipitated at 825 °C and grew at 850 °C. However, the corresponding XRD patterns (Fig. 2) revealed an amorphous nature. The discrepancy between the microstructure and the XRD patterns is possibly due to the small amount of the SBN phase formed in this temperature range. When the temperature was further increased (e.g. 900 and 1000 °C), a large amount of SBN phase and $B_2S_3$ phase formed. The highly etched matrix indicated that the $B_2S_3$ phase had crystallized from the residual-glass matrix, possibly because of the increased silicon content and decreased niobium content, which were established during the crystallization of SBN.

It is well known that glass powders densify by viscous coalescence. However, most crystallizable glass powders are difficult to sinter because of the large surface area for nucleation, promoting crystal growth from the surface of every glass particle toward the center and inhibiting effective sintering to achieve full density [24, 25]. In the present study, a very high degree of densification has been achieved at 825 °C (Fig. 1) before the remarkable crystallization from both of the surface and bulk regions of glass particle (at 875 °C, see Fig. 2). Therefore, SBN-containing glass-ceramics with high sintered densities can be obtained.

The dielectric properties of the samples with the higher sintered densities were investigated, as shown in Fig. 4(a) and (b). It can be seen from Fig. 4(a) that the dielectric constant ($k$) of the samples sintered at 800–850 °C was higher at low frequencies ($<$100 Hz) and drastically reduced to smaller than 50 at frequencies

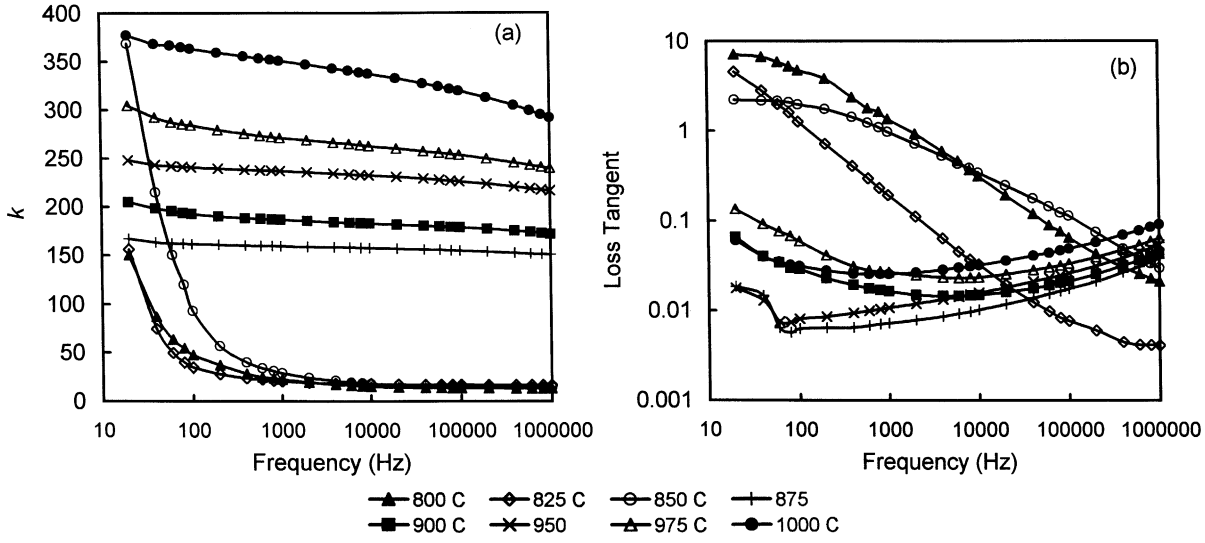


Fig. 4. (a) Dielectric constant and (b) dielectric loss tangent as a function of frequency for the samples sintered at 800–1000 °C.

>100 Hz. Because glass phase was the major phase in this temperature range, the higher dielectric constant at lower frequencies might be caused by space charge polarization in the glass phase [27]. When the sintering temperature was increased to 875 °C, considerable amount of SBN phase crystallized from the glass phase. Therefore, the characteristic of space charge effect at lower frequencies disappeared. The dielectric constant at higher frequencies remarkably increased, because of the high dielectric constant of SBN phase, to above than 150. When the sintering temperature was further increased, the dielectric constant increased, possibly due to the previously discussed increase in the SBN content. The maximum dielectric constant at 1 kHz is about 351 for the glass-ceramic sintered at 1000 °C.

According to Fig. 4(b), the dielectric loss tangent (tan$\delta$) for the samples sintered at lower temperatures (800–850 °C) was higher at lower frequencies. On the other hand, the tan$\delta$ values for the samples sintered at 875–1000 °C was low at lower frequencies (e.g., 0.7–2.7% at 1 kHz) and increased with the increasing frequency. There might be a peak of tan$\delta$ caused by ion jump relaxation [27] at frequency higher than 1 MHz.

The *P–E* hysteresis loop for the glass-ceramic sintered at 1000C, which showing the highest dielectric constant in the present study, was measured and shown in Fig. 5. The hysteresis loop revealed slim and some non-saturation, possibly because of the high coercive field which resulted in electrical breakdown before saturation was complete. Moreover, the existence of second phases

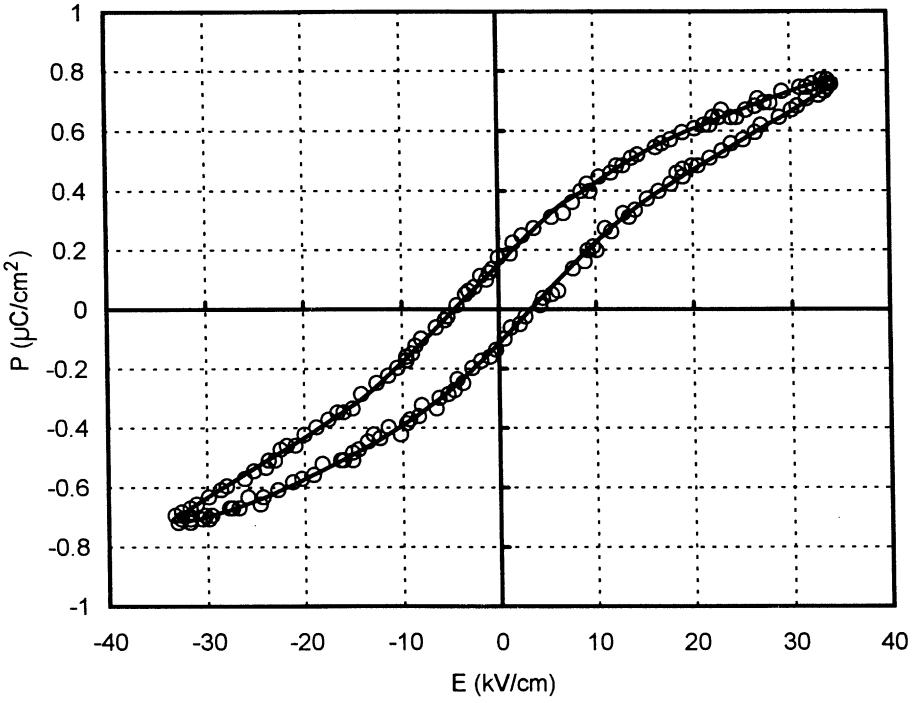


Fig. 5. *P–E* hysteresis loop at 60 Hz for the sample sintered at 1000 °C.

Table 1
Dielectric and ferroelectric properties the present glass-ceramic and some ferroelectric materials

| Materials | Properties | | | | Ref. |
|---|---|---|---|---|---|
| | $k$[a] | tan $\delta$[a] (%) | $P_r$ (μC/cm$^2$) | $E_c$ (kV/cm) | |
| $PbTiO_3$ glass-ceramic | 122 | 2.2 | 5.6 | 65 | 8 |
| PZT glass-ceramic | 61 | 1.3 | 0.94 | 12 | 8 |
| $(Sr,Ba)Nb_2O_6$ glass-ceramic (this study) | 351 | 2.5 | 0.15 | 4.5 | |
| $(Sr_{0.5}Ba_{0.5})Nb_2O_6$ ceramic | 1100 | 4.4 | ~2.6 | 3.7 | 28 |
| *$NaNbO_3$ glass-ceramic* | | | | | |
| Grain size = 0.2 μm | | | 0.2 | | 17 |
| Grain size = 1 μm | | | 0.8 | | 17 |
| *$BaTiO_3$ glass-ceramic* | | | | | |
| Prepared by a $BaO–TiO_2–B_2O_3$ glass | 2600 | 1.8 | ~0.8 | ~5 | 2 |
| Prepared by a $BaO–TiO_2–B_2O_3–SiO_2$ glass | 670 | 0.9 | ~0.2 | ~12.5 | 2 |

[a] 1 kHz.

($B_2S_3$ and residual glass), the small SBN grain-size, and the stresses applied by the surrounding rigid glass-matrix are also considered to be responsible for the observed non-saturated loop. However, the existence of ferroelectricity, which gives the most important pre-condition of the pyroelectricity and piezoelectricity, is confirmed for the present glass-ceramic. The dielectric and ferroelectric properties of the present glass-ceramic (sintered at 1000 °C) and some ferroelectric materials are summarized in Table 1. The value of the remanent polarization (*Pr*) for the present SBN glass-ceramic was about 0.15 μC/cm$^2$. This value is lower than that for lead-based perovskite glass-ceramics, and is near to that for some lead-free glass-ceramics. The coercive field (*Ec*) for the present glass-ceramic was about 4.5 kV/cm.

The further objective of this work is to develop glass-ceramics containing SBN as the single crystalline phase.

## 4. Conclusions

The densification, crystallization, and dielectric/ferroelectric properties of a $SrO–BaO–Nb_2O_5–SiO_2$ glass-ceramic were investigated. The following results have emerged:

1. (Sr, Ba)$Nb_2O_6$-containing glass-ceramic which is sinterable below 1000 °C can be obtained. The high sinterability is attributed to that the major crystallization process occurred after the sintering of the glass powder compact.
2. The primary and secondary crystalline phases were (Sr, Ba)$Nb_2O_6$ tungsten bronze and $Ba_2Si_3O_8$, respectively.
3. The dielectric constant increased with the increase in sintering temperature. The maximum dielectric constant at 1 kHz is about 351 for the glass-ceramic sintered at 1000 °C. The variations of dielectric properties with sintering temperature and frequency can be explained by the degree of SBN crystallization.
4. The existence of ferroelectricity is verified for the present glass-ceramic. The hysteresis loop shows slim and some non-saturation. The values of the remanent polarization and the coercive field were about 0.15 μC/cm$^2$ and 4.5 kV/cm, respectively, for the glass-ceramic sintered at 1000 °C.

## Acknowledgements

This work was supported by Tatung University under Contract No. B86-1707-01.

## References

[1] A. Herczog, Barrier layers in semiconducting barium titanate glass-ceramics, J. Am. Ceram. Soc. 67 (1984) 484–490.
[2] K. Yao, L. Zhang, X. Yao, W. Zhu, Preparation and properties of barium titanate glass-ceramics sintered from sol–gel-derived powders, J. Mater. Sci. 32 (1997) 3659–3665.
[3] D. McCauley, R.E. Newnham, C.A. Randall, Intrinsic size effects in a barium titanate glass-ceramic, J. Am. Ceram. Soc. 81 (1998) 979–987.
[4] A. Bhargava, J.E. Shelby, R.L. Snyder, Crystallization of glasses in the system $BaO–TiO_2–B_2O_3$, J. Non-Cryst. Solids 102 (1988) 136–142.
[5] T. Kokubo, M. Tashiro, Dielectric properties of fine-grained $PbTiO_3$ crystals precipitated in a glass, J. Non-Cryst. Solids 13 (1973/74) 328–340.
[6] S.M. Lynch, J.E. Shelby, Crystal clamping in lead titanate glass-ceramics, J. Am. Ceram. Soc. 67 (1984) 424–427.
[7] D.G. Grossman, J.O. Isard, The application of dielectric mixing formulae to glass-ceramic systems, J. Phys. D 3 (1970) 1058–1067.
[8] B. Houng, M.J. Haun, Lead titanate and lead zirconate titanate piezoelectric glass-ceramics, Ferroelectrics 154 (1994) 107–112.
[9] C.G. Bergeron, C.K. Russell, Nucleation and growth of lead titanate from a glass, J. Am. Ceram. Soc. 48 (1965) 115–118.
[10] W.K. Tredway, S.H. Risbud, C.G. Bergeron, Characterization of metastable phases preceding crystallization of a $PbO–SiO_2–TiO_2–Al_2O_3$ glass, in: J.H. Simmons, D.R. Uhlmann, G.H. Beall (Eds.), Advances in Ceramics, vol. 4, Nucleation and Crystallization in Glasses, The American Ceramic Society, Westerville, OH, 1982, pp. 163–168.
[11] D.E. Vernacotola, Alkali niobium and tantalum silicate glasses and ferroelectric glass-ceramics, in: J.E. Shelby (Ed.), Rare Eelements in Glasses, Trans Tech Publications Ltd, Switzerland, 1994, pp. 379–408.
[12] T. Komatsu, H.G. Kim, H. Mohri, Raman scattering study on local structures of $Te^{4+}$ and $Nb^{5+}$ in $LiNbO_3–TeO_2$ glasses, J. Mater. Sci. Lett. 15 (1996) 2026–2029.
[13] H.C. Zeng, K. Tanaka, K. Hirao, N. Soga, Crystallization and glass formation in $50Li_2O·50Nb_2O_5$ and $25Li_2O·25Nb_2O_5·50SiO_2$, J. Non-Cryst. Solids 209 (1997) 112–121.
[14] M. Todorović, Lj. Radonjić, Lithium-niobate ferroelectric material obtained by glass crystallization, Ceram. Int. 23 (1997) 55–60.
[15] M. Todorović, Lj. Radonjić, Ferroelectric solid solution crystals of the $ABO_3$ type by glass crystallization, in: P. Vincenzini (Ed.), Ceramics Today—Tomorrow's Ceramics, Elsevier, 1991, pp. 1999–2004.
[16] N.F. Borelli, Electrooptic effect in transparent niobate glass-ceramic systems, J. Appl. Phys. 38 (1967) 4243–4247.
[17] N.F. Borelli, M.M. Layton, Dielectric and optical properties of transparent ferroelectric glass-ceramic systems, J. Non-Cryst. Solids 6 (1971) 197–212.
[18] M.M. Layton, A. Herczog, Nucleation and crystallization of $NaNbO_3$ from glasses in the $Na_2O–Nb_2O_5SiO_2$ system, J. Am. Ceram. Soc. 50 (1967) 369–375.
[19] T. Komatsu, K. Shioya, K. Matusita, Fabrication of transparent tellurite glasses containing potassium niobate crystals by an incorporation method, J. Am. Ceram. Soc. 76 (1993) 2923–2926.
[20] T. Komatsu, J. Onuma, H.G. Kim, J.R. Kim, Formation of Rb-doped crystalline phase with second harmonic generation in transparent $K_2O–Nb_2O_5–TeO_2$ glass ceramics, J. Mater. Sci. Lett. 15 (1996) 2130–2133.
[21] M.J. Reece, C.A. Worrell, G.J. Hill, R. Morrell, Microstructures and dielectric properties of ferroelectric glass-ceramics, J. Am. Ceram. Soc. 79 (1996) 17–26.

[22] J.J. Shyu, J.R. Wang, Crystallization and dielectric properties of SrO–BaO–$Nb_2O_5$–$SiO_2$ tungsten-bronze glass-ceramics, J. Am. Ceram. Soc. 83 (2000) 3135–3140.
[23] E.M. Rabinovich, Review—preparation of glass by sintering, J. Mater. Sci. 20 (1985) 4259–4297.
[24] S.H. Knickerbocker, A.H. Kumar, L.W. Herron, Cordierite glass-ceramics for multilayer ceramic packaging, Am. Ceram. Soc. Bull. 72 (1993) 90–95.
[25] E.M. Rabinovich, Cordierite glass-ceramics produced by sintering, in: J.H. Simmons, D.R. Uhlmann, G.H. Beall (Eds.), Advances in Ceramics, vol. 4., Nucleation and Crystallization in Glasses, The American Ceramic Society, Columbus, OH, 1982, pp. 327–333.
[26] B. Ryu, I. Yasui, Sintering and crystallization behaviour of glass powder and block with a composition of anorthite and the microstructure dependence of its thermal expansion, J. Mater. Sci. 29 (1994) 3323–3328.
[27] W.D. Kingery, H.K. Bowen, D.R. Uhlmann, Introduction to Ceramics, second ed., John Wiley & Sons, Singapore, 1991.
[28] S.B. Deshpande, H.S. Potdar, P.D. Godbole, S.K. Date, Preparation and ferroelectric properties of SBN:50 ceramics, J. Am. Ceram. Soc. 75 (1992) 2581–2585.